Discrete DNA Reaction-Diffusion Model for Implementing Simple Cellular Automaton

Ibuki Kawamata[1(✉)], Satoru Yoshizawa[1], Fumi Takabatake[1], Ken Sugawara[2], and Satoshi Murata[1]

[1] Department of Robotics, School of Engineering, Tohoku University, Sendai, Japan
kawamata@molbot.mech.tohoku.ac.jp
[2] Department of Information Science, Faculty of Liberal Arts, Tohoku Gakuin University, Sendai, Japan

Abstract. We introduce a theoretical model of DNA chemical reaction-diffusion network capable of performing a simple cellular automaton. The model is based on well-characterized enzymatic bistable switch that was reported to work *in vitro*. Our main purpose is to propose an autonomous, feasible, and macro DNA system for experimental implementation.

As a demonstration, we choose a maze-solving cellular automaton. The key idea to emulate the automaton by chemical reactions is assuming a space discretized by hydrogel capsules which can be regarded as cells. The capsule is used both to keep the state uniform and control the communication between neighboring capsules.

Simulations under continuous and discrete space are successfully performed. The simulation results indicate that our model evolves as expected both in space and time from initial conditions. Further investigation also suggests that the ability of the model can be extended by changing parameters. Possible applications of this research include pattern formation and a simple computation. By overcoming some experimental difficulties, we expect that our framework can be a good candidate to program and implement a spatio-temporal chemical reaction system.

Keywords: DNA chemical reaction network · Cellular automaton · Spatio-temporal evolution · Pattern formation · Maze solving

1 Introduction

DNA is a suitable material to develop a system with desired structure and behavior because of its programmability. Elaborate systems from static structures to dynamic reactions have been reported [1–3]. For dynamic system that reacts in a single test tube, a variety of functionalities are demonstrated such as logic circuits, amplification, and oscillation [4–7]. Some DNA nano-structures can change their geometry in nano-scale precision [8].

Challenging topic of such dynamic systems is to increase the size to macro-scale [9,10]. One of the possible applications by scaling-up reactions is pattern

M. Amos and A. Condon (Eds.): UCNC 2016, LNCS 9726, pp. 168–181, 2016.
DOI: 10.1007/978-3-319-41312-9_14

formation. Common technique to achieve a pattern formation by chemical reaction is using a Turing pattern [11–13]. The technique is a good candidate to explain the patterns seen in nature [14], and worthy of future research.

Achieving simple patterns by DNA chemical reactions networks are demonstrated using UV stimulus or enzymatic reactions [15,16]. Since the reactions are limited in function, how to program a system with desired dynamics is of interest. For a well-mixed one-pot system, design principles have been addressed using abstractions and simulations of chemical reactions [8,17–19]. Recently, theoretical frameworks using both reaction and diffusion of DNA molecules for pattern formation and computation have also been reported [20–23].

To extend the programmability for one dimensional pattern formation, theoretical model that can emulate a cellular automaton by DNA was proposed [24]. Those theoretical models, however, consist of a huge chemical reaction network and seem to require large efforts of optimization when it comes to implement designed systems in real experiments. Furthermore, though the model of cellular automaton is well-designed and emulates an evolution of a specific cellular automaton, an external clock to control the phase of diffusion was assumed. A novel model that overcomes the problems and provides autonomous cellular automaton using simple and realistic chemical reactions may broaden the field of DNA computing.

In this paper, we propose a theoretical model of reaction diffusion system that implements a simple cellular automaton. The network employs an already well-characterized DNA bistable switch that is driven by enzyme reactions [25]. To discretize space, we assume a capsule of hydrogel that represents a single state of a cell [26,27]. While communication between capsules is done by slow diffusion, the concentration inside a capsule is ensured to be uniform by fast diffusion.

For the proof of concept, we formalize a concrete reaction-diffusion model and simulate the behavior of the model from some initial states. The introduced cellular automaton is capable of solving a maze. Inspired by a research using cellular automaton as a computation platform [28], we further discuss how to compute a simple deterministic finite automaton by our system.

2 Discrete Model

2.1 Transition Rules

We decide to emulate a simple cellular automaton that can solve a maze from specific initial state [29]. The automaton is related to a problem of routing and an example representation of the system was proposed [30]. First, we illustrate the discrete model of the cellular automaton.

Cells of the cellular automaton are arranged in a square lattice. Each cell has either state 'a' or state 'b', which represent wall and path, respectively. The transition rules are quite simple that only the state 'b' can switch to 'a' as shown in Fig. 1. A cell communicates only with four neighboring cells in north, south, east, and west.

A cell counts the number of neighboring cells in state 'a' and decides its transition. If the number is less than or equal to two, it keeps its state. Otherwise, the state changes from 'b' to 'a'.

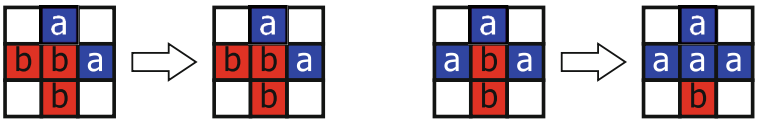

(a) Case of two neighbors (b) Case of three neighbors

Fig. 1. The transition rules. A cell in state 'b' does not change its state if the number of neighboring cells in state 'a' is less than or equal to two. The cell switches to 'a', however, if there are 3 or more neighboring cells in state 'a'. Blue and red cells represents states 'a' and 'b', respectively. (Color figure online)

2.2 Example Simulation

As an example of the cellular automaton, we simulated a system from specific initial state using a software platform called "Ready" [31] (Fig. 2). Since the transition rules eliminate a path at a dead end, the route from the starting to the ending cells is preserved. Although the transition rules are very simple, the simulation result indicates that the cellular automaton is capable of computing a routing problem.

The model is still far from chemical reactions because all the state, space, and time are discrete in the model. In contrast, chemical reaction works under continuous concentration, space, and time. We have to link the gap between discrete and continuous systems.

3 Continuous Model

3.1 Bistable System

To discretize state, we make use of a bistable switch which is chemically implemented and verified by an *in vitro* experiment [25]. The switch is composed of signal DNA, template DNA, and enzymes (Fig. 3(a)). We illustrate single stranded DNA (ssDNA) as an arrow corresponding to the direction from 5' to 3' ends of phosphate backbone, which is a customary way of representing DNA.

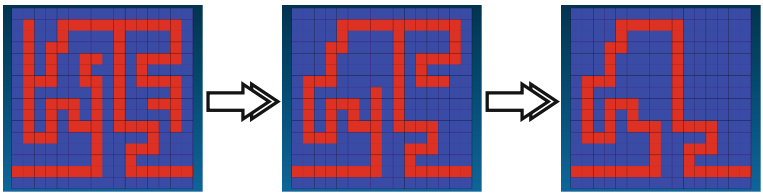

Fig. 2. The simulation of maze solving cellular automaton. Three frames of the simulation result are shown. Transition rules are adopted by a synchronized manner.

The signals are unmodified ssDNAs, which are named as 'a', 'b', 'inha', and 'inhb'. The templates are chemically modified ssDNAs that program the interactions between signals. The program is executed by collaborative reactions of polymerase and nickase. Since exonuclease decomposes signal strands, the state of the system is in a dynamic equilibration.

The switch has one of the two states, where either ssDNA 'a' or 'b' has higher concentration. If the concentration of 'a' is high, that of 'b' is very low, and vice versa. The dynamics are programmed by exclusive amplification reactions, whose topological interactions are explained in Fig. 3(b). The switch is capable of changing its state from one to the other by adding excess amount of the competitive strand.

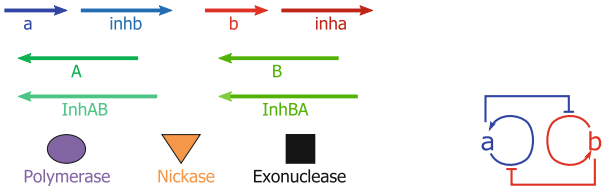

(a) DNA and enzymes

(b) Topological representation

Fig. 3. Schematic of the bistable switch. (a) DNA strands and enzymes necessary for the bistable switch are summarized. Signal and templates strands are represented by right- and left- pointing arrows, respectively. We name each strand by the string below the strand. The reactions of the system are driven by three enzymes that are polymerase, nickase, and exonuclease. Using signal strands a and b as primers, templates A and B can produce DNA strands a and b in an autocatalytic manner, respectively. Templates InhAB and InhBA can also produce signal strands inhb and inha using a and b as primers, respectively. Produced inha and inhb hybridize to templates A and B, which will prevent the autocatalytic production of a and b, respectively. (b) Topological representation of the system. Though the signal 'a' and 'b' produces themselves by auto-catalytic reactions, they inhibit the production of one another (Color figure online).

We list some features of the switch as below.

- We can discretize a state of the solution even when the concentration of molecules is continuous.
- It is possible to switch the state of the solution from 'b' to 'a'.
- Detailed ordinary differential equations (ODEs) and a parameter set are given.
- The system is experimentally simple and reliable.

3.2 Capsule of Hydrogel

To discretize space, we think of encapsulating the switch in a hydrogel capsule. The capsule has a shell of hydrogel and core of solution (Fig. 4(a)). Since the hydrogel is a buffer fixed by a polymer network, small molecules can diffuse slowly. A molecule that is larger than the pore size of the network, however, cannot pass through the hydrogel. Of course, all the molecules diffuse relatively fast in a solution and the concentration of molecules inside a capsule becomes uniform.

An idea to prevent the template strands, which encode the state of the switch, from diffusing is necessary. We propose to attach molecules such as large DNA structure or other polymer [32] to the 5' ends of the templates strands. Those assumptions guarantee that one cell has only one state, while signal strands can diffuse to neighboring cells. The space is made by arranging such capsules in a square lattice (Fig. 4(b)).

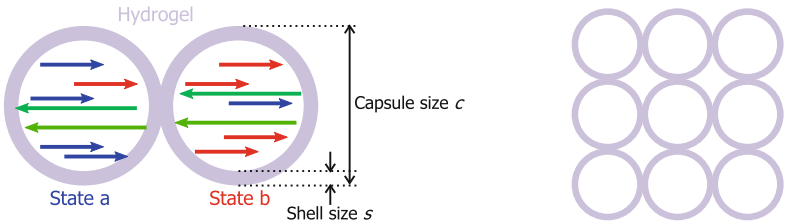

(a) Hydrogel capsules

(b) Lattice of capsules

Fig. 4. Concept of hydrogel capsules. (a) Hydrogel capsules contain DNA strands for the switch. Enzymes are assumed to be distributed in all the area, though they are not shown. The left and right capsules are in state 'a' and 'b', respectively. The size of the capsule is represented by two length parameters c and s. (b) The capsules are arranged in square lattice, where capsules are contacting by the hydrogel shell. One capsule has four neighboring capsules to match the model of the cellular automaton (Color figure online).

4 Reaction Diffusion Model

We formalized reaction diffusion equations with 26 variables and 19 parameters summarized in the Appendix A. The ODEs and kinetic parameters were taken from the detailed model of the original bistable switch [25,33]. The only difference is the terms of diffusion for diffusing molecular species.

Following the names of each structure of the original article, the variables were assigned to all the signal strands, templates strands, and possible intermediate structures. The parameters include rate constant, Michaelis-Menten constants, and diffusion coefficients. Note that state 'a' is more favorable than state 'b' due to the difference of the kinetic constants such as denaturation of DNA.

Since the speed of diffusion is different between gel and solution, the term of diffusion is formalized by an inner product of the differential operator ∇. We roughly estimated the diffusion coefficients of DNA in solution and hydrogel from experimental data [34,35].

To be a concrete model, we assumed that the capsule is made of liquid-core and a 1.5 % alginate hydrogel shell [36]. We fixed the ratio between capsule size c and the thickness of the shell s to be $c = 8s$. We used $s = 200\,\mu\text{m}$ as a default value unless otherwise specified.

5 Simulation Results

5.1 Continuous Space

First we simulated the system under continuous space to prove that the transition rules are possible to achieve. All the results were obtained by coding the system for the reaction-diffusion simulator "Ready" [31]. In practice, the space was represented by a square lattice with total 1872 grids.

By numerically solving the equations from defined initial states with nine cells, we observed expected transitions of the states of the cells (Fig. 5(a),(b)). We further changed the parameter of shell thickness s and the initial concentrations of template strands and checked if the desired state transitions happened. As shown in the phase diagram (Fig. 5(d)), those conditions crucially affected the result of transition.

5.2 Discrete Space

Since the continuous space simulation was computationally expensive, we discretize the space to simulate a larger space. In the modified model for the discrete space, we ignored the diffusion coefficients in solution and only took into account those in hydrogel shell. As a result, we have successfully simulated the spatio-temporal evolution of the maze problem (Fig. 6) using "Ready" [31] again. Although the space was discrete, the concentrations of each molecule were simulated by continuous ODEs. The result strongly indicates that the DNA system with our assumptions can perform a simple computation written in a cellular automaton.

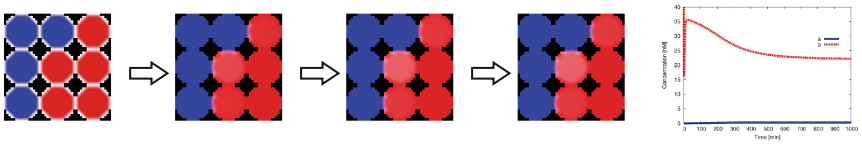

(a) Two neighbors

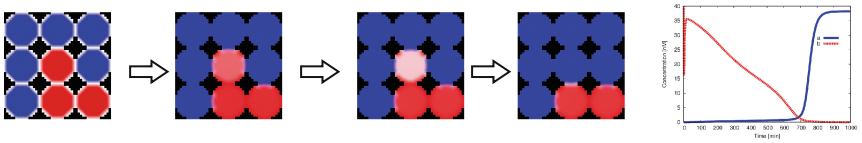

(b) Three neighbors

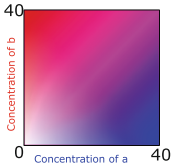

(c) Color map

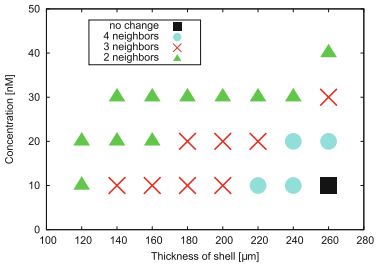

(d) Phase diagram

Fig. 5. Simulation results under continuous space. If the initial state of a cell was 'a' and 'b', concentration of the corresponding signal strands of the core was set to 40 nM, respectively. One capsule was represented by a circle with 16 grids in diameter. Initial concentrations of the template strands were 20 nM in every place. Other signal strands and intermediate structures had 0 nM as an initial condition. As shown in (c), blue and red channels correspond to the concentrations of strand 'a' and 'b', respectively. (a) When a cell had two neighbors that were in state 'a', the state did not change. Time evolutions of the concentrations of signal strands in the center cell are shown in the right graph. X and y axes are time in minutes and concentration in nM. (b) The same simulation result for the three neighbors. In this case, the state changed from 'b' to 'a'. (d) Phase diagram of transitions condition. The result is a summary of simulations (for 1000 min) by varying the shell size and initial concentrations of templates strands. The desired transition occurred only when the conditions of cross mark were satisfied. The legend of the diagram indicates the minimum number of neighbors for the state transition. (Color figure online)

After some simulations, we found that the rule is not limited to solve mazes. It was possible to carry other types of simulations (Fig. 7). Specifically, we performed the simulations of forming unique pattern, starting from a random initial

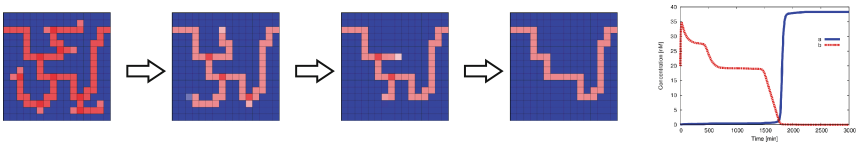

Fig. 6. Simulation result of the maze problem under discrete space. Distance between cells was changed to 650 µm. We used 20 nM as initial concentrations of signal and templates strands. Similar to the continuous simulation, time evolutions of the concentrations are shown. For the time evolution, we selected the cell that changed the number of neighbors in state 'a' for three times.

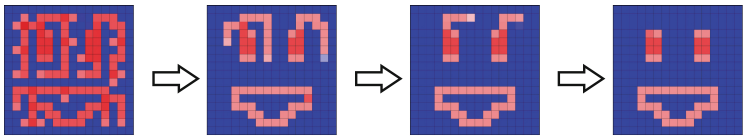

(a) Specific initial pattern

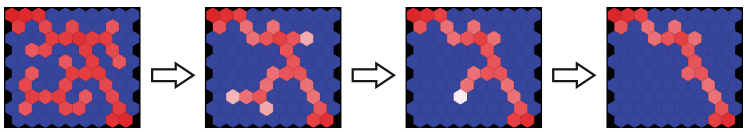

(b) Honeycomb lattice

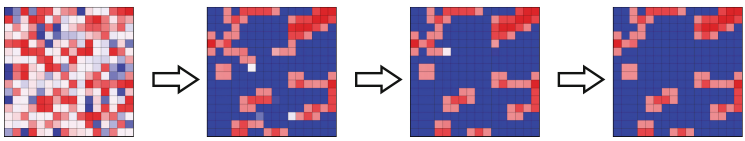

(c) Random initial pattern

Fig. 7. Other simulation results (a) As a first demonstrations, we simulated a smile face from a specific initial pattern. (b) By changing the cell distance to 900 µm in a honeycomb lattice, the transition rules slightly changed. The state 'b' changed to 'a' when there are 5 or more neighboring cells in state 'a'. (c) In the case of random initial pattern.

pattern, and assuming a hexagonal lattice. The first simulation result suggests the application of our framework for other pattern formation problem.

The second and third simulations were carried in consideration of experimental implementation. It may be difficult to arrange the capsules in a square lattice nor write a complex initial pattern. Those results suggest that our framework can be easily extended depending on the experimental demands.

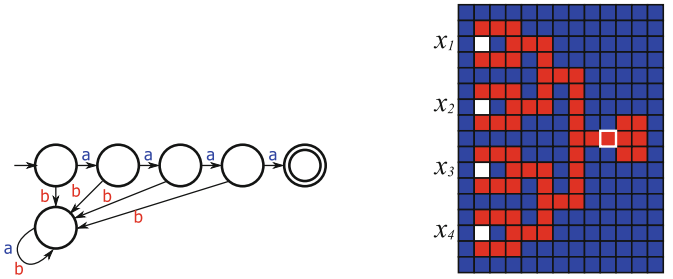

(a) Automaton that accepts only "aaaa"

(b) Program that corresponds the automaton

Fig. 8. State transition machine and its implementation as an initial state of the cellular automaton. (a) A schematic representation of an automaton that reads sequence of letters and accepts four sequential 'a'. (b) The program of the maze solving cellular automaton is shown as an initial state. Four empty cells are painted according to the four letters $x_1 \cdots x_4$. If the sequence is acceptable, the marked cell changes its state as a result of applying the rules.

6 Application and Discussion

We introduce an application of the maze solving cellular automaton from the computational viewpoint. Since the transition only occurs from states 'b' to 'a', the ability of the cellular automaton seems extremely limited. However, it is possible to program a very simple state transition machine as an initial state. For example, an automaton that accepts four sequential 'a' can be programmed (Fig. 8).

Although it treats finite number of letters, the concept of using such cellular automata for computational purpose is comprehensive. Challenging problems for further research may include how to design a feasible chemical reaction network that can emulate a Turing universal cellular automaton like the game of life [37]. Candidates to extend the ability of our framework is to adopt the techniques to design DNA chemical reaction networks described in Sect. 1. From the results of our and other theoretical models [24], it looks still difficult to overcome the trade-off between the ability of computation and the network complexity in terms of the number of molecular species.

Finally, we point out some technical difficulties we are aware of when implementing our system in real experiments. The alginate hydrogel contains calcium as a cross-linker, which may affect the kinetics of enzymes used in the system. If we have to avoid the alginate hydrogel, other polymer that has the same ratio between the scale of the capsule and diffusion coefficients must substitute the shell. Formation of uniform hydrogel capsules and arranging them in a desired lattice is also of problem. Writing the initial pattern may be achieved by modifying DNA with a photo-responsive molecule [38].

The energy source to drive the reactions is important. We assumed that sufficient substrates such as dNTPs are provided at the initial state. If the reaction time becomes long, it may be necessary to supply them from external bath.

In this paper, we propose a theoretical reaction-diffusion model that is based on well-characterized DNA and enzyme reactions. We numerically simulate the model and show the capability to emulate a maze-solving cellular automaton. The important idea is to encapsulate molecules in hydrogel capsules that is arranged in a lattice. Unlike the conventional theoretical model capable of emulating a cellular automaton by DNA chemical reaction network, our model does not require external clock and evolves autonomously. Our framework contributes to aid the experimental implementation of feasible DNA chemical reaction-diffusion network for pattern formation and computation.

Acknowledgement. We appreciate Masami Hagiya to motivate this research. Helpful advice from the experimental viewpoints were given by Hiroyuki Asanuma, Takashi Arimura, Yusuke Hara, and Nobuyoshi Miyamoto. We thank Teijiro Isokawa and Ferdinand Peper for discussion including the suggestion to simulate a normal automaton by a cellular automaton. This research was supported by Grant-in-Aid for Scientific Research on Innovative Areas "Molecular Robotics" (No. 24104005) and Grant-in-Aid for Young Scientists (Start-up, 26880002).

A Reaction diffusion model

The equations of our model are shown below. Terms for diffusion, which we added to the original equations, are highlighted by red color.

$$\begin{aligned}
\frac{\partial}{\partial t}[\mathrm{a}] =& \nabla \cdot (D_{\mathrm{fast}} \nabla [\mathrm{a}]) + k_{\mathrm{d}}^{\mathrm{a}} \times ([\mathrm{aA}] + [\mathrm{Aa}] + 2 \times [\mathrm{aAa}] + [\mathrm{aInhAB}] + [\mathrm{aInhABinhb}]) + k_{\mathrm{h}} \times [\mathrm{inha}] \times ([\mathrm{aA}] + [\mathrm{Aa}]) \\
& - k_{\mathrm{h}} \times [\mathrm{a}] \times (2 \times [\mathrm{A}] + [\mathrm{aA}] + [\mathrm{Aa}] + 2 \times \mathit{toe} \times [\mathrm{Ainh}] + [\mathrm{InhAB}] + [\mathrm{InhABinhb}]) \\
& + k_{\mathrm{pol,sd}} \times [\mathrm{aAa}] / K_{\mathrm{m,sd}} / C_{\mathrm{pol}} - k_{\mathrm{exo}} \times [\mathrm{a}] / K_{\mathrm{m,input}} / C_{\mathrm{exo}} \\
\frac{\partial}{\partial t}[\mathrm{b}] =& \nabla \cdot (D_{\mathrm{fast}} \nabla [\mathrm{b}]) + k_{\mathrm{d}}^{\mathrm{b}} \times ([\mathrm{bB}] + [\mathrm{Bb}] + 2 \times [\mathrm{bBb}] + [\mathrm{bInhBA}] + [\mathrm{bInhBAinha}]) + k_{\mathrm{h}} \times [\mathrm{inhb}] \times ([\mathrm{bB}] + [\mathrm{Bb}]) \\
& - k_{\mathrm{h}} \times [\mathrm{b}] \times (2 \times [\mathrm{B}] + [\mathrm{bB}] + [\mathrm{Bb}] + 2 \times \mathit{toe} \times [\mathrm{Binh}] + [\mathrm{InhBA}] + [\mathrm{InhBAinha}]) \\
& + k_{\mathrm{pol,sd}} \times [\mathrm{bBb}] / K_{\mathrm{m,sd}} / C_{\mathrm{pol}} - k_{\mathrm{exo}} \times [\mathrm{b}] / K_{\mathrm{m,input}} / C_{\mathrm{exo}} \\
\frac{\partial}{\partial t}[\mathrm{A}] =& \nabla \cdot (D_{\mathrm{slow}} \nabla [\mathrm{A}]) + k_{\mathrm{d}}^{\mathrm{a}} \times ([\mathrm{aA}] + [\mathrm{Aa}]) + k_{\mathrm{d}}^{\mathrm{inha}} \times [\mathrm{Ainh}] - k_{\mathrm{h}} \times [\mathrm{A}] \times (2 \times [\mathrm{a}] + [\mathrm{inha}]) \\
\frac{\partial}{\partial t}[\mathrm{B}] =& \nabla \cdot (D_{\mathrm{slow}} \nabla [\mathrm{B}]) + k_{\mathrm{d}}^{\mathrm{b}} \times ([\mathrm{bB}] + [\mathrm{Bb}]) + k_{\mathrm{d}}^{\mathrm{inhb}} \times [\mathrm{Binh}] - k_{\mathrm{h}} \times [\mathrm{B}] \times (2 \times [\mathrm{b}] + [\mathrm{inhb}])
\end{aligned}$$

$$
\begin{aligned}
\frac{\partial}{\partial t}[\mathrm{aA}] =& \nabla\cdot(D_{\mathrm{slow}}\nabla[\mathrm{aA}]) + k_{\mathrm{h}}\times[\mathrm{a}]\times([\mathrm{A}]-[\mathrm{aA}]) + k_{\mathrm{h}}\times \mathit{toe}\times[\mathrm{a}]\times[\mathrm{Ainh}] + k_{\mathrm{d}}^{\mathrm{a}}\times[\mathrm{aAa}] \\
& - k_{\mathrm{h}}\times[\mathrm{inha}]\times[\mathrm{aA}] - k_{\mathrm{d}}^{\mathrm{a}}\times[\mathrm{aA}] - k_{\mathrm{pol}}\times[\mathrm{aA}]/K_{\mathrm{m}}/C_{\mathrm{pol}} \\
\frac{\partial}{\partial t}[\mathrm{bB}] =& \nabla\cdot(D_{\mathrm{slow}}\nabla[\mathrm{bB}]) + k_{\mathrm{h}}\times[\mathrm{b}]\times([\mathrm{B}]-[\mathrm{bB}]) + k_{\mathrm{h}}\times \mathit{toe}\times[\mathrm{b}]\times[\mathrm{Binh}] + k_{\mathrm{d}}^{\mathrm{b}}\times[\mathrm{bBb}] \\
& - k_{\mathrm{h}}\times[\mathrm{inhb}]\times[\mathrm{bB}] - k_{\mathrm{d}}^{\mathrm{b}}\times[\mathrm{bB}] - k_{\mathrm{pol}}\times[\mathrm{bB}]/K_{\mathrm{m}}/C_{\mathrm{pol}} \\
\frac{\partial}{\partial t}[\mathrm{Aa}] =& \nabla\cdot(D_{\mathrm{slow}}\nabla[\mathrm{Aa}]) + k_{\mathrm{h}}\times[\mathrm{a}]\times([\mathrm{A}]-[\mathrm{Aa}]) + k_{\mathrm{h}}\times \mathit{toe}\times[\mathrm{a}]\times[\mathrm{Ainh}] + k_{\mathrm{d}}^{\mathrm{a}}\times[\mathrm{aAa}] \\
& - k_{\mathrm{h}}\times[\mathrm{inha}]\times[\mathrm{Aa}] - k_{\mathrm{d}}^{\mathrm{a}}\times[\mathrm{Aa}] \\
\frac{\partial}{\partial t}[\mathrm{Bb}] =& \nabla\cdot(D_{\mathrm{slow}}\nabla[\mathrm{Bb}]) + k_{\mathrm{h}}\times[\mathrm{b}]\times([\mathrm{B}]-[\mathrm{Bb}]) + k_{\mathrm{h}}\times \mathit{toe}\times[\mathrm{b}]\times[\mathrm{Binh}] + k_{\mathrm{d}}^{\mathrm{b}}\times[\mathrm{bBb}] \\
& - k_{\mathrm{h}}\times[\mathrm{inhb}]\times[\mathrm{Bb}] - k_{\mathrm{d}}^{\mathrm{b}}\times[\mathrm{Bb}] \\
\frac{\partial}{\partial t}[\mathrm{aAa}] =& \nabla\cdot(D_{\mathrm{slow}}\nabla[\mathrm{aAa}]) + k_{\mathrm{h}}\times[\mathrm{a}]\times([\mathrm{aA}]+[\mathrm{Aa}]) - 2\times k_{\mathrm{d}}^{\mathrm{a}}\times[\mathrm{aAa}] \\
& + k_{\mathrm{nick}}\times[\mathrm{Aaa}]/K_{\mathrm{nick}} - k_{\mathrm{pol,sd}}\times[\mathrm{aAa}]/K_{\mathrm{m,sd}}/C_{\mathrm{pol}} \\
\frac{\partial}{\partial t}[\mathrm{bBb}] =& \nabla\cdot(D_{\mathrm{slow}}\nabla[\mathrm{bBb}]) + k_{\mathrm{h}}\times[\mathrm{b}]\times([\mathrm{bB}]+[\mathrm{Bb}]) - 2\times k_{\mathrm{d}}^{\mathrm{b}}\times[\mathrm{bBb}] \\
& + k_{\mathrm{nick}}\times[\mathrm{Bbb}]/K_{\mathrm{nick}} - k_{\mathrm{pol,sd}}\times[\mathrm{bBb}]/K_{\mathrm{m,sd}}/C_{\mathrm{pol}} \\
\frac{\partial}{\partial t}[\mathrm{Aaa}] =& \nabla\cdot(D_{\mathrm{slow}}\nabla[\mathrm{Aaa}]) + k_{\mathrm{pol}}\times[\mathrm{aA}]/K_{\mathrm{m}}/C_{\mathrm{pol}} + k_{\mathrm{pol,sd}} \\
& \times[\mathrm{aAa}]/K_{\mathrm{m,sd}}/C_{\mathrm{pol}} - k_{\mathrm{nick}}\times[\mathrm{Aaa}]/K_{\mathrm{nick}} \\
\frac{\partial}{\partial t}[\mathrm{Bbb}] =& \nabla\cdot(D_{\mathrm{slow}}\nabla[\mathrm{Bbb}]) + k_{\mathrm{pol}} \\
& \times[\mathrm{bB}]/K_{\mathrm{m}}/C_{\mathrm{pol}} + k_{\mathrm{pol,sd}}\times[\mathrm{bBb}]/K_{\mathrm{m,sd}}/C_{\mathrm{pol}} - k_{\mathrm{nick}}\times[\mathrm{Bbb}]/K_{\mathrm{nick}} \\
\frac{\partial}{\partial t}[\mathrm{inha}] =& \nabla\cdot(D_{\mathrm{fast}}\nabla[\mathrm{inha}]) + k_{\mathrm{d}}^{\mathrm{inha}}\times([\mathrm{Ainh}]+[\mathrm{InhBAinha}]+[\mathrm{bInhBAinha}]) \\
& - k_{\mathrm{h}}\times[\mathrm{inha}]\times([\mathrm{InhBA}]+[\mathrm{bInhBA}]+[\mathrm{A}]+[\mathrm{aA}]+[\mathrm{Aa}]) \\
& + k_{\mathrm{pol,sd}}\times[\mathrm{bInhBAinha}]/K_{\mathrm{m,sd}}/C_{\mathrm{pol}} - k_{\mathrm{exo}}\times[\mathrm{inha}]/K_{\mathrm{m,inh}}/C_{\mathrm{exo}} \\
\frac{\partial}{\partial t}[\mathrm{inhb}] =& \nabla\cdot(D_{\mathrm{fast}}\nabla[\mathrm{inhb}]) + k_{\mathrm{d}}^{\mathrm{inhb}}\times([\mathrm{Binh}]+[\mathrm{InhABinhb}]+[\mathrm{aInhABinhb}]) \\
& - k_{\mathrm{h}}\times[\mathrm{inhb}]\times([\mathrm{InhAB}]+[\mathrm{aInhAB}]+[\mathrm{B}]+[\mathrm{bB}]+[\mathrm{Bb}]) \\
& + k_{\mathrm{pol,sd}}\times[\mathrm{aInhABinhb}]/K_{\mathrm{m,sd}}/C_{\mathrm{pol}} - k_{\mathrm{exo}}\times[\mathrm{inhb}]/K_{\mathrm{m,inh}}/C_{\mathrm{exo}} \\
\frac{\partial}{\partial t}[\mathrm{Ainh}] =& \nabla\cdot(D_{\mathrm{slow}}\nabla[\mathrm{Ainh}]) + k_{\mathrm{h}}\times[\mathrm{inha}]\times([\mathrm{A}]+[\mathrm{aA}]+[\mathrm{Aa}]) - 2 \\
& \times k_{\mathrm{h}}\times \mathit{toe}\times[\mathrm{a}]\times[\mathrm{Ainh}] - k_{\mathrm{d}}^{\mathrm{inha}}\times[\mathrm{Ainh}] \\
\frac{\partial}{\partial t}[\mathrm{Binh}] =& \nabla\cdot(D_{\mathrm{slow}}\nabla[\mathrm{Binh}]) + k_{\mathrm{h}}\times[\mathrm{inhb}]\times([\mathrm{B}]+[\mathrm{bB}]+[\mathrm{Bb}]) - 2 \\
& \times k_{\mathrm{h}}\times \mathit{toe}\times[\mathrm{b}]\times[\mathrm{Binh}] - k_{\mathrm{d}}^{\mathrm{inhb}}\times[\mathrm{Binh}] \\
\frac{\partial}{\partial t}[\mathrm{InhAB}] =& \nabla\cdot(D_{\mathrm{slow}}\nabla[\mathrm{InhAB}]) + k_{\mathrm{d}}^{\mathrm{a}}\times[\mathrm{aInhAB}] + k_{\mathrm{d}}^{\mathrm{inhb}}\times[\mathrm{InhABinhb}] - k_{\mathrm{h}}\times[\mathrm{InhAB}]\times([\mathrm{a}]+[\mathrm{inhb}]) \\
\frac{\partial}{\partial t}[\mathrm{InhBA}] =& \nabla\cdot(D_{\mathrm{slow}}\nabla[\mathrm{InhBA}]) + k_{\mathrm{d}}^{\mathrm{b}}\times[\mathrm{bInhBA}] + k_{\mathrm{d}}^{\mathrm{inha}}\times[\mathrm{InhBAinha}] - k_{\mathrm{h}}\times[\mathrm{InhBA}]\times([\mathrm{b}]+[\mathrm{inha}]) \\
\frac{\partial}{\partial t}[\mathrm{aInhAB}] =& \nabla\cdot(D_{\mathrm{slow}}\nabla[\mathrm{aInhAB}]) + k_{\mathrm{h}}\times[\mathrm{a}]\times[\mathrm{InhAB}] - k_{\mathrm{h}}\times[\mathrm{aInhAB}]\times[\mathrm{inhb}] + k_{\mathrm{d}}^{\mathrm{inhb}}\times[\mathrm{aInhABinhb}] \\
& - k_{\mathrm{d}}^{\mathrm{a}}\times[\mathrm{aInhAB}] - k_{\mathrm{pol}}\times[\mathrm{aInhAB}]/K_{\mathrm{m}}/C_{\mathrm{pol}} \\
\frac{\partial}{\partial t}[\mathrm{bInhBA}] =& \nabla\cdot(D_{\mathrm{slow}}\nabla[\mathrm{bInhBA}]) + k_{\mathrm{h}}\times[\mathrm{b}]\times[\mathrm{InhBA}] - k_{\mathrm{h}}\times[\mathrm{bInhBA}]\times[\mathrm{inha}] + k_{\mathrm{d}}^{\mathrm{inha}}\times[\mathrm{bInhBAinha}] \\
& - k_{\mathrm{d}}^{\mathrm{b}}\times[\mathrm{bInhBA}] - k_{\mathrm{pol}}\times[\mathrm{bInhBA}]/K_{\mathrm{m}}/C_{\mathrm{pol}} \\
\frac{\partial}{\partial t}[\mathrm{InhABinhb}] =& \nabla\cdot(D_{\mathrm{slow}}\nabla[\mathrm{InhABinhb}]) + k_{\mathrm{h}}\times[\mathrm{inhb}]\times[\mathrm{InhAB}] - k_{\mathrm{h}}\times[\mathrm{InhABinhb}]\times[\mathrm{a}] \\
& + k_{\mathrm{d}}^{\mathrm{a}}\times[\mathrm{aInhABinhb}] - k_{\mathrm{d}}^{\mathrm{inhb}}\times[\mathrm{InhABinhb}] \\
\frac{\partial}{\partial t}[\mathrm{InhBAinha}] =& \nabla\cdot(D_{\mathrm{slow}}\nabla[\mathrm{InhBAinha}]) + k_{\mathrm{h}}\times[\mathrm{inha}]\times[\mathrm{InhBA}] - k_{\mathrm{h}}\times[\mathrm{InhBAinha}]\times[\mathrm{b}] \\
& + k_{\mathrm{d}}^{\mathrm{b}}\times[\mathrm{bInhBAinha}] - k_{\mathrm{d}}^{\mathrm{inha}}\times[\mathrm{InhBAinha}]
\end{aligned}
$$

$$
\begin{aligned}
\frac{\partial}{\partial t}[\mathrm{aInhABinhb}] &= \nabla\cdot(D_{\mathrm{slow}}\nabla[\mathrm{aInhABinhb}]) + k_{\mathrm{h}}\times[\mathrm{a}]\times[\mathrm{InhABinhb}] + k_{\mathrm{h}}\times[\mathrm{aInhAB}]\times[\mathrm{inhb}] - k_{\mathrm{d}}^{\mathrm{a}}\times[\mathrm{aInhABinhb}] \\
&\quad - k_{\mathrm{d}}^{\mathrm{inhb}}\times[\mathrm{aInhABinhb}] + k_{\mathrm{nick}}\times[\mathrm{InhABainhb}]/K_{\mathrm{nick}} - k_{\mathrm{pol,sd}}\times[\mathrm{aInhABinhb}]/K_{\mathrm{m,sd}}/C_{\mathrm{pol}} \\
\frac{\partial}{\partial t}[\mathrm{bInhBAinha}] &= \nabla\cdot(D_{\mathrm{slow}}\nabla[\mathrm{bInhBAinha}]) + k_{\mathrm{h}}\times[\mathrm{b}]\times[\mathrm{InhBAinha}] + k_{\mathrm{h}}\times[\mathrm{bInhBA}]\times[\mathrm{inha}] - k_{\mathrm{d}}^{\mathrm{b}}\times[\mathrm{bInhBAinha}] \\
&\quad - k_{\mathrm{d}}^{\mathrm{inha}}\times[\mathrm{bInhBAinha}] + k_{\mathrm{nick}}\times[\mathrm{InhBAbinha}]/K_{\mathrm{nick}} - k_{\mathrm{pol,sd}}\times[\mathrm{bInhBAinha}]/K_{\mathrm{m,sd}}/C_{\mathrm{pol}} \\
\frac{\partial}{\partial t}[\mathrm{InhABainhb}] &= \nabla\cdot(D_{\mathrm{slow}}\nabla[\mathrm{InhABainhb}]) + k_{\mathrm{pol}}\times[\mathrm{aInhAB}]/K_{\mathrm{m}}/C_{\mathrm{pol}} + k_{\mathrm{pol,sd}}\times[\mathrm{aInhABinhb}]/K_{\mathrm{m,sd}}/C_{\mathrm{pol}} \\
&\quad - k_{\mathrm{nick}}\times[\mathrm{InhABainhb}]/K_{\mathrm{nick}} \\
\frac{\partial}{\partial t}[\mathrm{InhBAbinha}] &= \nabla\cdot(D_{\mathrm{slow}}\nabla[\mathrm{InhBAbinha}]) + k_{\mathrm{pol}}\times[\mathrm{bInhBA}]/K_{\mathrm{m}}/C_{\mathrm{pol}} + k_{\mathrm{pol,sd}}\times[\mathrm{bInhBAinha}]/K_{\mathrm{m,sd}}/C_{\mathrm{pol}} \\
&\quad - k_{\mathrm{nick}}\times[\mathrm{InhBAbinha}]/K_{\mathrm{nick}},
\end{aligned}
$$

where

$$
\begin{aligned}
C_{\mathrm{pol}} &= 1 + [\mathrm{aA}]/K_{\mathrm{m}} + [\mathrm{bB}]/K_{\mathrm{m}} + [\mathrm{aAa}]/K_{\mathrm{m,sd}} + [\mathrm{bBb}]/K_{\mathrm{m,sd}} \\
&\quad + [\mathrm{aInhAB}]/K_{\mathrm{m}} + [\mathrm{bInhBA}]/K_{\mathrm{m}} + [\mathrm{aInhABinhb}]/K_{\mathrm{m,sd}} + [\mathrm{bInhBAinha}]/K_{\mathrm{m,sd}} \\
C_{\mathrm{exo}} &= 1 + [\mathrm{a}]/K_{\mathrm{m,input}} + [\mathrm{b}]/K_{\mathrm{m,input}} + [\mathrm{inhb}]/K_{\mathrm{m,inh}} + [\mathrm{inha}]/K_{\mathrm{m,inh}} \\
K_{\mathrm{nick}} &= K_{\mathrm{mn}} + [\mathrm{Aaa}] + [\mathrm{Bbb}] + [\mathrm{InhABainhb}] + [\mathrm{InhBAbinha}].
\end{aligned}
$$

As kinetic parameters, we used the fitted values of the original article [25]. Diffusion coefficient of DNA in solution was roughly estimated from experimental values [34,35].

$$
\begin{aligned}
&k_{\mathrm{h}} = 0.06[\mathrm{nM}^{-1}\cdot\mathrm{min}^{-1}],\ k_{\mathrm{d}}^{\mathrm{a}} = k_{\mathrm{h}}/0.013[\mathrm{min}^{-1}],\ k_{\mathrm{d}}^{\mathrm{b}} = k_{\mathrm{h}}/0.0045[\mathrm{min}^{-1}], \\
&k_{\mathrm{d}}^{\mathrm{inha}} = k_{\mathrm{h}}/5.3[\mathrm{min}^{-1}],\ k_{\mathrm{d}}^{\mathrm{inhb}} = k_{\mathrm{h}}/1.3[\mathrm{min}^{-1}],\ toe = 0.01, \\
&k_{\mathrm{pol}} = 2100[\mathrm{nM}\cdot\mathrm{min}^{-1}],\ k_{\mathrm{pol,sd}} = 420[\mathrm{nM}\cdot\mathrm{min}^{-1}],\ k_{\mathrm{nick}} = 80[\mathrm{nM}\cdot\mathrm{min}^{-1}],\ k_{\mathrm{exo}} = 300[\mathrm{nM}\cdot\mathrm{min}^{-1}], \\
&K_{\mathrm{m}} = 80[\mathrm{nM}],\ K_{\mathrm{m,sd}} = 5.5[\mathrm{nM}],\ K_{\mathrm{mn}} = 30[\mathrm{nM}],\ K_{\mathrm{m,input}} = 440[\mathrm{nM}],\ K_{\mathrm{m,inh}} = 150[\mathrm{nM}].
\end{aligned}
$$

$$
D_{\mathrm{fast}} = \begin{cases} 1.2\times10^{-8} & [\mathrm{m}^2\cdot\mathrm{min}^{-1}]\ \text{(in solution)} \\ 6.0\times10^{-10} & [\mathrm{m}^2\cdot\mathrm{min}^{-1}]\ \text{(in hydrogel)} \end{cases}, \qquad D_{\mathrm{slow}} = \begin{cases} 1.2\times10^{-8} & [\mathrm{m}^2\cdot\mathrm{min}^{-1}]\ \text{(in solution)} \\ 3.0\times10^{-12} & [\mathrm{m}^2\cdot\mathrm{min}^{-1}]\ \text{(in hydrogel)} \end{cases}
$$

References

1. Rangnekar, A., LaBean, T.H.: Building DNA nanostructures for molecular computation, templated assembly, and biological applications. Acc. Chem. Res. **47**(6), 1778–1788 (2014)
2. Zhang, F., Nangreave, J., Liu, Y., Yan, H.: Structural DNA nanotechnology: state of the art and future perspective. J. Am. Chem. Soc. **136**(32), 11198–11211 (2014)
3. Zhang, D.Y., Seelig, G.: Dynamic DNA nanotechnology using strand-displacement reactions. Nat. Chem. **3**(2), 103–113 (2011)
4. Seelig, G., Soloveichik, D., Zhang, D.Y., Winfree, E.: Enzyme-free nucleic acid logic circuits. Science **314**(5805), 1585–1588 (2006)
5. Qian, L., Winfree, E.: Scaling up digital circuit computation with DNA strand displacement cascades. Science **332**(6034), 1196–1201 (2011)
6. Turberfield, A.J., Yurke, B.: Engineering entropy-driven reactions and networks catalyzed by DNA. Science **318**(5853), 1121–1125 (2007)
7. Fujii, T., Rondelez, Y.: Predator-prey molecular ecosystems. ACS Nano **7**(1), 27–34 (2013)

8. Kuzuya, A., Ohya, Y.: Nanomechanical molecular devices made of DNA origami. Acc. Chem. Res. **47**(6), 1742–1749 (2014)
9. Murata, S., Konagaya, A., Kobayashi, S., Saito, H., Hagiya, M.: Molecular robotics: a new paradigm for artifacts. New Gener. Comput. **31**, 27–45 (2013)
10. Hagiya, M., Konagaya, A., Kobayashi, S., Saito, H., Murata, S.: Molecular robots with sensors and intelligence. Acc. Chem. Res. **47**(6), 1681–1690 (2014)
11. Turing, A.M.: The chemical basis of morphogenesis. Philos. Trans. R. Soc. B Biol. Sci. **237**(641), 37–72 (1952)
12. Lee, K.-J., McCormick, W.D., Pearson, J.E., Swinney, H.L.: Experimental observation of self-replicating spots in a reaction-diffusion system. Nature **369**(6477), 215–218 (1994)
13. Vanag, V.K., Epstein, I.R.: Tomography of reaction-diffusion microemulsions reveals three-dimensional turing patterns. Science **331**(1309), 1309–1312 (2011)
14. Kondo, S., Miura, T.: Reaction-diffusion model as a framework for understanding biological pattern formation. Science **329**(5999), 1616–1620 (2010)
15. Chirieleison, S.M., Allen, P.B., Simpson, Z.B., Ellington, A.D., Chen, X.: Pattern transformation with DNA circuits. Nat. Chem. **5**(12), 1000–1005 (2013)
16. Padirac, A., Fujii, T., Estévez-Torres, A., Rondelez, Y.: Spatial waves in synthetic biochemical networks. J. Am. Chem. Soc. **135**(39), 14586–14592 (2013)
17. Soloveichik, D., Seelig, G., Winfree, E.: DNA as a universal substrate for chemical kinetics. Proc. Nat. Acad. Sci. **107**(12), 5393–5398 (2010)
18. Phillips, A., Cardelli, L.: A programming language for composable DNA circuits. J. R. Soc. Interface **6**(Suppl 4), S419–S436 (2009)
19. Aubert, N., Mosca, C., Fujii, T., Hagiya, M., Rondelez, Y.: Computer-assisted design for scaling up systems based on DNA reaction networks. J. R. Soc. Interface **11**(93), 20131167 (2014)
20. Allen, P.B., Chen, X., Simpson, Z.B., Ellington, A.D.: Modeling scalable pattern generation in DNA reaction networks. Artif. Life **13**, 441–448 (2012). http://dx.doi.org/10.7551/978-0-262-31050-5-ch058
21. Scalise, D., Schulman, R.: Designing modular reaction-diffusion programs for complex pattern formation. Technology **02**(01), 55–66 (2014)
22. Dalchau, N., Seelig, G., Phillips, A.: Computational design of reaction-diffusion patterns using DNA-based chemical reaction networks. In: Murata, S., Kobayashi, S. (eds.) DNA 2014. LNCS, vol. 8727, pp. 84–99. Springer, Heidelberg (2014)
23. Hagiya, M., Wang, S., Kawamata, I., Murata, S., Isokawa, T., Peper, F., Imai, K.: On DNA-based gellular automata. In: Ibarra, O.H., Kari, L., Kopecki, S. (eds.) UCNC 2014. LNCS, vol. 8553, pp. 177–189. Springer, Heidelberg (2014)
24. Scalise, D., Schulman, R.: Emulating cellular automata in chemical reaction-diffusion networks. In: Murata, S., Kobayashi, S. (eds.) DNA 2014. LNCS, vol. 8727, pp. 67–83. Springer, Heidelberg (2014)
25. Padirac, A., Fujii, T., Rondelez, Y.: Bottom-up construction of in vitro switchable memories. Proc. Nat. Acad. Sci. **109**(47), E3212–E3220 (2012)
26. Fischlechner, M., Schaerli, Y., Mohamed, M.F., Patil, S., Abell, C., Hollfelder, F.: Evolution of enzyme catalysts caged in biomimetic gel-shell beads. Nat. Chem. **6**(9), 791–796 (2014)
27. Machado, A.H., Lundberg, D., Ribeiro, A.J., Veiga, F.J., Miguel, M.G., Lindman, B., Olsson, U.: Encapsulation of DNA in macroscopic and nanosized calcium alginate gel particles. Langmuir. **29**(51), 15926–15935 (2013)
28. Cook, M.: Universality in elementary cellular automata. Complex Syst. **15**, 1–40 (2004)

29. Nayfeh, B.A.: Cellular automata for solving mazes. Dr. Dobb's J. **18**(2), 32–38 (1993)
30. Saber, M.A., Mirenkov, N.: A visual representation of cellular automata-like systems. J. Visual Lang. Comput. **15**(6), 409–438 (2004)
31. Hutton, T., Munafo, R., Trevorrow, A., Rokicki, T., Wills, D.: Ready, a cross-platform implementation of various reaction-diffusion systems. https://github.com/GollyGang/ready
32. Allen, P., Chen, X., Ellington, A.: Spatial control of DNA reaction networks by DNA sequence. Molecules **17**(12), 13390–13402 (2012)
33. Zhang, D.Y., Winfree, E.: Control of DNA strand displacement kinetics using toehold exchange. J. Am. Chem. Soc. **131**(47), 17303–17314 (2009)
34. Stellwagen, E., Yongjun, L., Stellwagen, N.C.: Unified description of electrophoresis and diffusion for DNA and other polyions. Biochemistry **42**(40), 11745–11750 (2003)
35. Pluen, A., Netti, P.A., Jain, R.K., Berk, D.A.: Diffusion of macromolecules in agarose gels: comparison of linear and globular configurations. Biophys. J. **77**(1), 542–552 (1999)
36. Bremond, N., Santanach-Carreras, E., Chu, L.-Y., Bibette, J.: Formation of liquid-core capsules having a thin hydrogel membrane: liquid pearls. Soft Matter **6**(11), 2484–2488 (2010)
37. Rendell, P.: Turing universality of the game of life. In: Adamatzky, A. (ed.) Collision-Based Computing, pp. 513–539. Springer, London (2002)
38. Feng, L., Romulus, J., Li, M., Sha, R., Royer, J., Kun-Ta, W., Qin, X., Seeman, N.C., Weck, M., Chaikin, P.: Cinnamate-based DNA photolithography. Nat. Mater. **12**, 747–753 (2013)